

Plasma-Assisted Chemical Vapor Deposition and Characterization of Boron Nitride Films

S. V. Nguyen and T. Nguyen

IBM Microelectronics, Hopewell Junction, New York 12533

H. Treichel

Siemens Components, IBM Facility, Essex Junction, Vermont 05452

O. Spindler

Siemens AG, Process Engineering and Support, 8000 München 83, Germany

ABSTRACT

Boron nitride films were deposited in a single-wafer plasma enhanced chemical vapor deposition (PECVD) system using two different reactant gas chemistries: (i) dilute diborane (1% B_2H_6 in nitrogen), nitrogen and ammonia; (ii) borazine ($B_3N_3H_6$), and nitrogen as precursor materials. Variations of deposition rates, thickness uniformities, refractive indexes, wet and plasma dry etch rates, film stress, and electrical properties were studied as a function of the corresponding deposition parameters. Several analytical methods such as Fourier transform infrared spectroscopy, x-ray photoelectron spectroscopy, nuclear reaction analysis, elastic recoil detection analysis, scanning and transmission electron microscopy were used to study the deposited films. Electrical properties were measured using metal-insulator-metal and metal-insulator-semiconductor structures. The stable boron nitride films do not react with water vapor showing dielectric constant values between 4.0 and 4.7. These good insulators also show promising characteristics for potential applications in high-performance ultralarge scale integration fabrication.

To enhance switching performance in ultralarge scale integrated (ULSI) devices, low dielectric constant (d.c.) insulators are needed to reduce the wiring capacitance between interlevel metals. Plasma boron nitride and silicon boron nitride films have been deposited¹⁻⁹ and studied as low dielectric constant materials for bipolar devices¹⁻⁷ and also as hard coating materials.⁹ Various chemical precursors such as borane-amine-hydrocarbon complexes,² diborane- BCl_3 -ammonia,^{1-7,9} and borazine⁸ have been used for film deposition. Recent publications^{7,10} show that the d.c. of boron nitride can be varied from 2.7 to 7.7 depending on deposition conditions and measurement methods. For ULSI fabrication, boron nitride films show excellent potential as chemical mechanical polishing (CMP) stop for global planarization.¹¹ This paper presents results of IBM and Siemens laboratories collaborative efforts in evaluating the plasma deposition and physical characterization of stable boron nitride films deposited in single-wafer plasma chemical vapor deposition (CVD) systems. Two different reactant gas chemistries are used for the deposition: (i) dilute diborane (1% B_2H_6 in nitrogen), nitrogen, and ammonia; (ii) borazine ($B_3N_3H_6$) and nitrogen as precursor materials. The results showed that stable boron nitride films can be deposited by both reactant gas chemistries, although slightly different film properties are obtained.

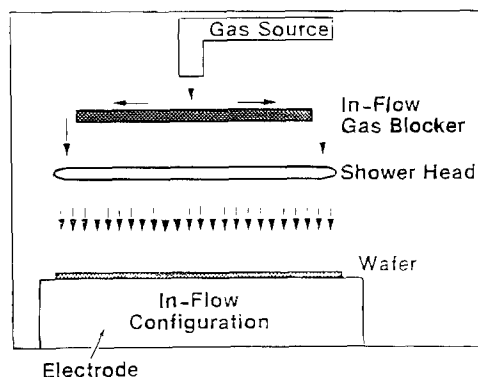


Fig. 1. Plasma CVD system for boron nitride deposition.

Experimental

Boron nitride films were deposited on silicon wafer in single-wafer plasma CVD system (13.6 MHz RF) with a shower-head gas distribution blocker and 180 cm² electrode area at 100 to 400°C,¹² as shown in Fig. 1. All of the precursors are of ultrahigh purity (99.999%). Typical deposition conditions for both chemistries are shown in Table I. Variations of film deposition rates, thickness uniformities, refractive indexes, and stress were studied as a function of various deposition process parameters such as pressure, power density, substrate temperature, and flow rates.

The physical and chemical properties of the deposited films were analyzed using ellipsometry (Gärtner AutoEL, He-Ne wavelength: 633 nm, and Plasmas at 633 and 1335 nm), Auger electron spectroscopy (AES; Physical Electronic Auger spectrometer), Fourier transform infrared spectroscopy (FTIR; Biorad) and x-ray photoelectron spectroscopy (XPS; Hewlett Packard, Model 5950B), scanning electron microscopy (SEM; Hitachi Instruments), and buffered HF etching (BHF).

Nuclear reaction analysis (NRA), elastic recoil detection analysis (ERDA; High Voltage Engineering, Type EN), Rutherford backscattering (RBS; High Voltage Engineering, Type AN2500), were used to determine the boron to nitrogen ratio and to measure the hydrogen concentration. Transmission electron microscopy (TEM; Siemens) and selected area electron diffraction (SAED) were also used to specify the crystallinity phases of the material.

A 7:4:1 buffered HF solution was prepared by mixing 7 volume (vol) of HNO_3 with 4 vol H_2O and 1 vol buffered HF. The 1 vol buffered HF solution was prepared by mixing

Table I. Typical deposition conditions for plasma boron nitride.

Precursor/process parameters	B_2H_6/NH_3	Borazine: $B_3N_3H_6/N_2$
B_2H_6 -flow (1% in N_2)	1800 sccm	—
Borazine flow	—	100 sccm
NH_3 flow	120 sccm	—
N_2 flow	4200 sccm	200 sccm
Electrode spacing	250 mils = 0.6 cm	380 mils = 0.95 cm
RF power	500 W	200 W
Process pressure	5 Torr = 660 Pa	3 Torr = 400 Pa
Susceptor temperature	400°C	300°C

Table II. Comparison of film properties B₂H₆/NH₃/N₂ vs. borazine/boron nitride.

	B ₂ H ₆ /NH ₃	Borazine: B ₃ N ₃ H ₆ /N ₂
Deposition rate	300 nm/min	370 nm/min
Uniformity	<5 to 10% (6σ)	±3% (3σ)
Reference index	1.746	1.732
Stress	-4×10^8 Pa = -4×10^9 dynes/cm ²	-1.5×10^8 Pa = -1.5×10^9 dynes/cm ²
Etch rate RIE	62 nm/min	28 nm/min
Etch rate H ₃ PO ₄ (167°C)	1 to 11 nm/h	—
Etch rate BHF	0.5 nm/min	<1 nm/min
B/N ratio	1.02	1.02
Hydrogen content	<8 a/o	<8 a/o
Density	1.89 g/cm ³	1.904 g/cm ³
Optical bandgap	4.7 eV	4.9 eV
Step coverage	60% (1 × 1 μm)	80% (0.5 × 0.5 μm)
Structure	Amorphous	Amorphous
Dielectric constant	3.8-5.7	3.8 to 5.7
Breakdown potential	6 to 7 MV/cm	6 to 8 MV/cm

10 vol of NH₄F (40%) and 1 vol HF (49%). The etch solution temperatures were maintained constantly at 25°C for buffered HF and 167°C for hot phosphoric acid during the wet etch tests.

The layers for AES (5 to 100 nm thickness) were sputtered by 1.5 keV Ar⁺ ions at 30 s intervals with rastered mode on a 100 μm² spot size to assess the composition with depth. To reduce the inhomogeneous sputtering effect, the ion beam was rastered for all sputter cleaning processes also. The boron and nitrogen concentrations were normal-

ized to an atomic ratio of 1:1 with a detection limit of about 1 atomic percent (a/o).

The surface and depth profile composition were analyzed by XPS with a detection limit of 1 a/o. The spectra were obtained using an aluminum Kα x-ray source with a monochromator. The atomic weight fractions were calculated from the integrated areas using a Scofield table¹³ and clean, thermally grown silicon oxide as reference. In addition, survey spectra were obtained for all films to assess for impurities and irregularities.

RBS with a detection limit of better than 0.1 a/o was used in addition to AES and XPS to reduce the error in composition analysis of the light element boron. Here, He⁺ ions (2 MeV) are scattered elastically in surface regions of the samples. The loss in energy allows simultaneous element identification and depth profiling.

NRA and ERDA were used to analyze the hydrogen. NRA was carried out at the State University of New York at Albany. The ¹⁵N depth profiling is a highly accurate precision technique for measuring concentration profiles of hydrogen in solids¹⁴ according to the nuclear reaction

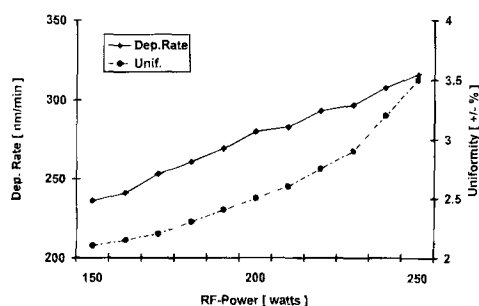
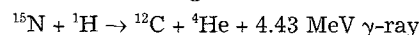


Fig. 2. Deposition rate and uniformity of BN vs. RF power (borazine chemistry).

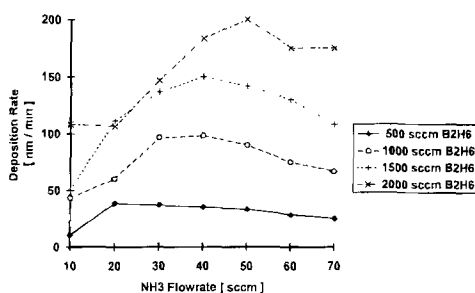


Fig. 3. Deposition rate and uniformity of BN vs. NH₃-flow (hydride chemistry).

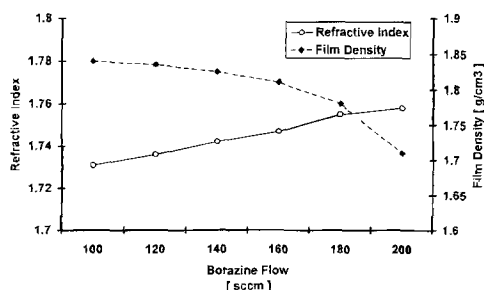


Fig. 4. Refractive index and film density of BN vs. borazine flow.

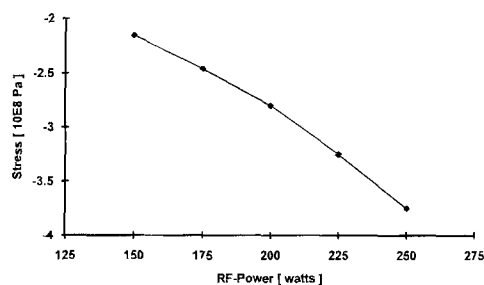


Fig. 5. Intrinsic stress of boron nitride vs. RF power (borazine chemistry).

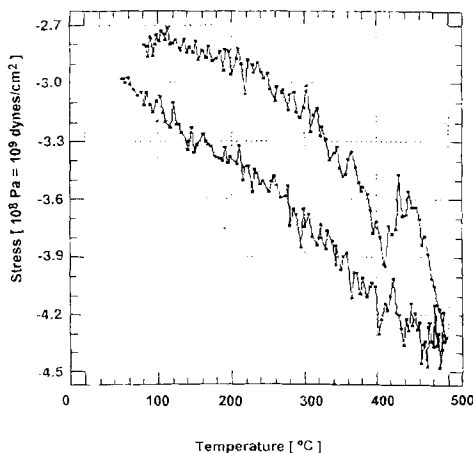


Fig. 6. Intrinsic stress of boron nitride vs. temperature (borazine chemistry).

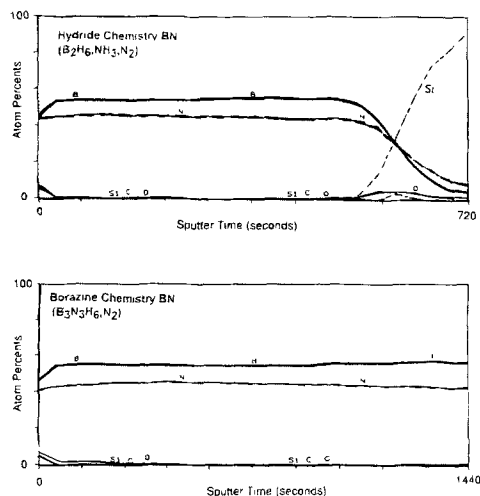


Fig. 7. XPS depth profiles of boron nitride.

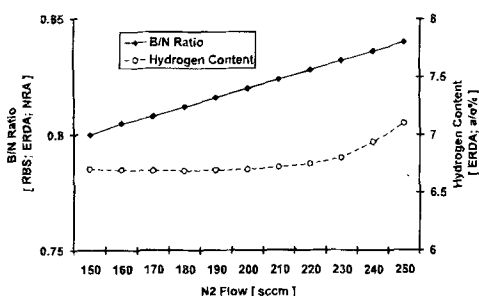


Fig. 8. B/N ratio and hydrogen content of BN vs. nitrogen flow (borazine chemistry).

In this reaction, the amount of γ -ray emission is proportional to the hydrogen concentration in the film bulk. It should be noted that the NRA technique determines both bonded (N-H, B-H) and trapped hydrogen (molecular or atomic) in the films without distinguishing the bonding structure. Therefore, the hydrogen concentration re-

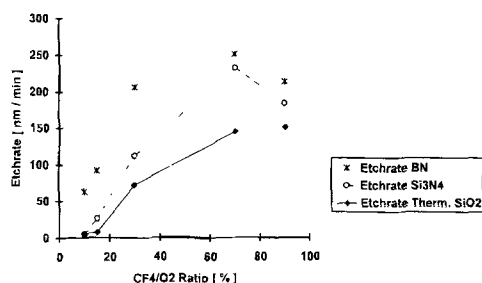


Fig. 9. Etch rates of BN, Si₃N₄, and thermal SiO₂ vs. CF₄/O₂ ratio (hydride chemistry).

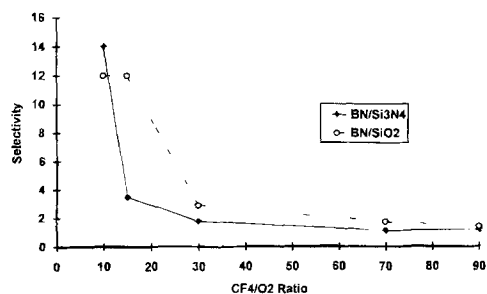


Fig. 10. Selectivity of boron nitride to Si₃N₄, and thermal SiO₂ vs. CF₄/O₂ ratio (hydride chemistry).

Table III. Magnetically enhanced etching conditions.

Process conditions	Values
Etch time	60 s
Pressure	80 mTorr = 10 Pa
Cathode temperature	20°C
RF power	400 W
Magnetic field	20 gauss
Gas flows (sccm)	2-18 CF ₄ (variable) 2-18 O ₂ (variable)
Etchtool	AME 5000

Table IV. Etch rate and selectivity of BN films in various CF₄/O₂ gas mixtures.

CF ₄ /O ₂ ratio (%)	Etch rate (nm/min)/selectivity				
	BN	LPCVD Si ₃ N ₄	Selectivity BN/Si ₃ N ₄	Thermal SiO ₂	Selectivity BN/SiO ₂
10	63.2	4.6	14:1	5.2	12:1
15	92.1	26.3	3.5:1	7.4	12:1
30	206.3	112.7	1.8:1	72.0	2.9:1
70	250.3	231.7	1.1:1	114.6	1.7:1
90	212.6	182.9	1.2:1	150.2	1.4:1

sults appear slightly higher than those obtained by other methods.

The strength of ERDA is the ability to analyze light elements in conjunction with depth profiling. Here, the elastic backscattering of elements such as Cl at 30 MeV allows a nondestructive determination without influencing the film bonding matrix and chemical states of the elements in the layers.

The boron nitride films deposited on silicon substrate were etched in a magnetron enhanced reactive ion etching (MERIE) system described in a previous publication.¹⁵ The plasma dry etch rates R were determined using laser interferometry. The etch rate, R , was calculated with the formula $R = \lambda / (2nt)$, where λ is the wavelength of the laser, n is the refractive index, and t is the etch time that changes the reflected intensity by one cycle.

SEM cross sections were taken to study the step coverage of the films over submicron (1.0 × 1.0 μ m) structures. TEM, especially selected area electron diffraction (SAED), determined the degree of crystallinity and what kind of crystalline phases are observed.

For metal insulator semiconductor (MIS) and metal insulator metal (MIM) electrical measurements at various frequencies, films of 10 to 100 nm thickness were deposited at 300 and 400°C on p-type silicon wafers with and without 7 nm of thermally grown silicon oxide films. The native oxide on the back side of the wafers was removed, and aluminum or gold electrodes evaporated onto the deposited films. Blanket aluminum on the back side of the wafers assured good contact of the counterelectrodes. Quasistatic and dynamic high frequency (1 MHz) C-V measurements (Hewlett Packard HP4274, Multifrequency LCR Meter) were used to find out the flatband voltage and breakdown strength. Capacitance values from C-V curves in a wider range of applied voltage to determine the true accumulation region were back-calculated for dielectric constant values ϵ_r , according to the following equation: $\epsilon_r = (C_p \times t) / (\epsilon_p \times A)$, where C_p is the measured capacitance, t is insulator thickness, ϵ_p is vacuum permittivity (8.854 × 10⁻¹⁴ F/cm), and A is the measured area. Other details of this electrical measurement have also been described in a recent report.¹⁶

Results and Discussions

The typical overall properties of the boron nitride films deposited by both processes (see Table I) are summarized in Table II. The layers, deposited under the conditions of Table I, have excellent thickness uniformities (6 sigma < 5 to 10%; Fig. 2). The deposition rate was calculated by dividing the measured mean thickness by the time of the corresponding deposition. Increasing RF power will increase the deposition rate (Fig. 2), whereas for diborane deposi-

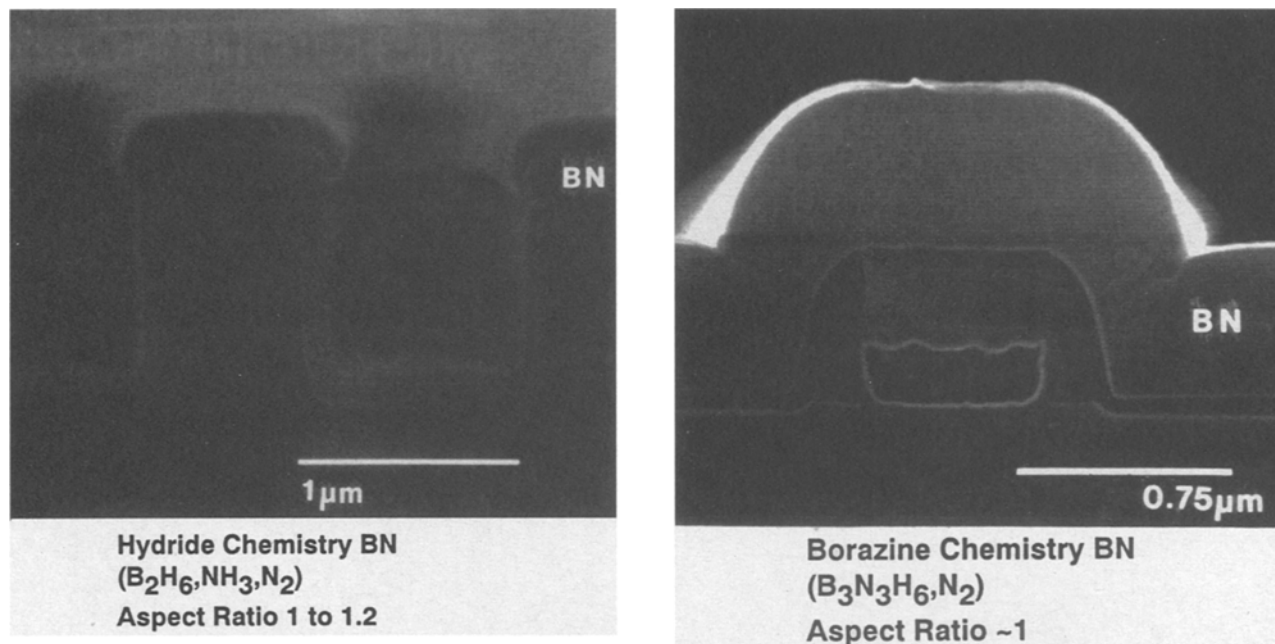


Fig. 11. Step coverage of BN (500 nm steps).

tion chemistry, increases of ammonia and diborane flow rates raise deposition rates marginally (Fig. 3). Nitrogen flow rates have a small effect. Increases in RF power density or, *e.g.*, borazine flow, are also increasing refractive indexes (Fig. 4). For both deposition chemistries, stable boron nitride films have refractive indexes ranging from 1.68 to 1.8, depending on deposition conditions.

The deposited boron nitride films have a lower density ρ ($\rho = 1.6$ to 1.9 g/cm³, Fig. 4) than the conventional bulk value of both hexagonal BN ($\rho = 2.2$ g/cm³) or cubic BN ($\rho = 3.4$ g/cm³)¹⁷ as determined by x-ray reflectometry.

The layers exhibit compressive stress in the range of -2×10^8 to -4×10^8 Pa, depending on deposition conditions (Fig. 5). During a subsequent heat-treatment (25 to 500°C) film stress increases by about a factor of 2, and relaxes during cool-down to the original value (Fig. 6). The measured stress values are generated using optical stress measurement (Flexus).

XPS and FTIR analyses show that boron nitride films deposited by hydride chemistry with a low $\text{NH}_3/\text{B}_2\text{H}_6$ ratio (<5) are boron-rich. These films are highly hygroscopic and oxidize readily in air or hot water vapor ambients. This is also the case for borazine chemistry deposition with high borazine/nitrogen flow ratio (>1) or at high RF power densities (>2.0 W/cm²).

Boron nitride films deposited with higher $\text{NH}_3/\text{B}_2\text{H}_6$ ratios (>5) (diborane chemistry) and a 2:1 nitrogen/borazine flow ratio are more stable with near stoichiometric composition (55 a/o B, 45 a/o N) with good depth thickness uniformity, as analyzed by AES. No oxygen or carbon contaminations are observed in the films bulk except for a small

amount near the surfaces and at the boron nitride/silicon substrate interfaces (Fig. 7). The oxygen and carbon observed at the silicon surface and the BN/silicon interface are due to oxygen and carbon absorption on silicon substrate prior to deposition.

These films are highly stable and show no reaction with 100°C water vapor or boiling water for 60 min time elapsed. After these films are annealed at 850°C in oxygen ambient for 30 min, only minimal surface oxidation (2 to 3 nm) were

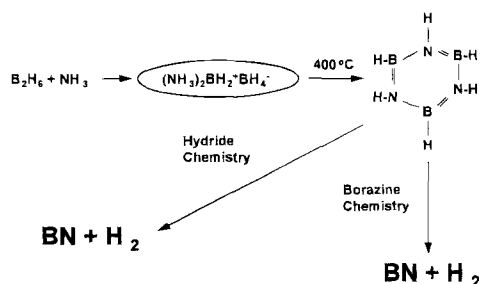


Fig. 12. Reaction steps and intermediates in plasma BN deposition.

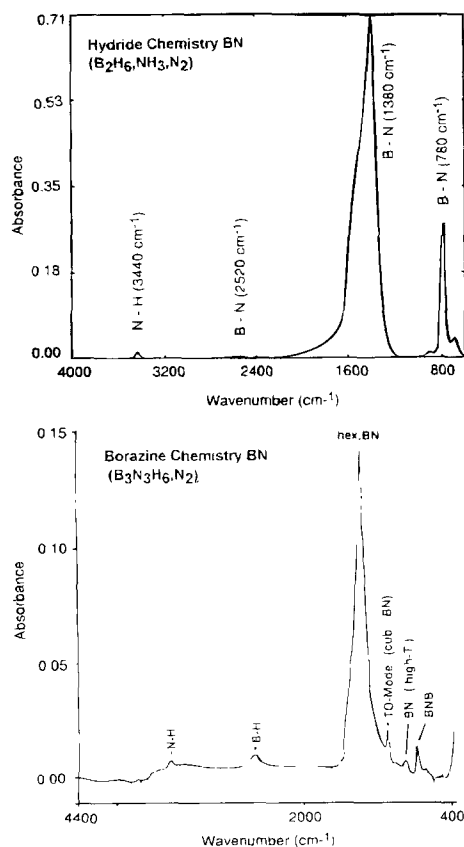


Fig. 13. FTIR spectra of BN (hydride chemistry) and of BN (borazine chemistry) as-deposited.

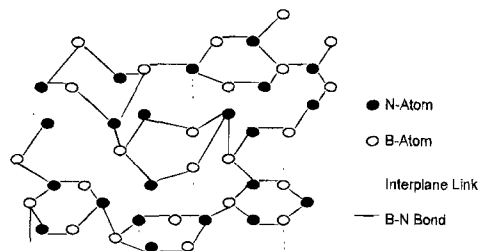


Fig. 14. Defect structure of borazine BN.

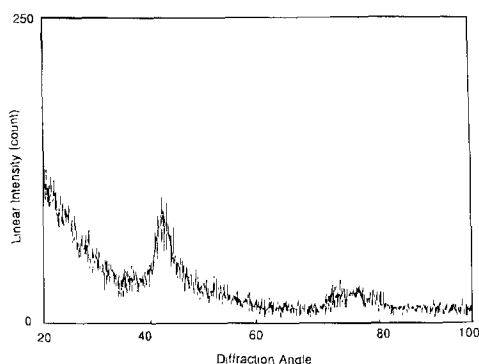


Fig. 15. XRD pattern of borazine BN.

observed. The films are also stable in nitrogen ambient annealing up to 950°C for 60 min.

NRA and ERDA analyses show that films deposited at higher $\text{NH}_3/\text{B}_2\text{H}_6$ ratios (>7) have less than 8 a/o hydrogen incorporation in the film, while films deposited with no or lower NH_3 flow have more hydrogen incorporated. The correlation of B/N ratio and hydrogen content varies, *e.g.*, with nitrogen flow (Fig. 8). The increase of the B/N ratio with

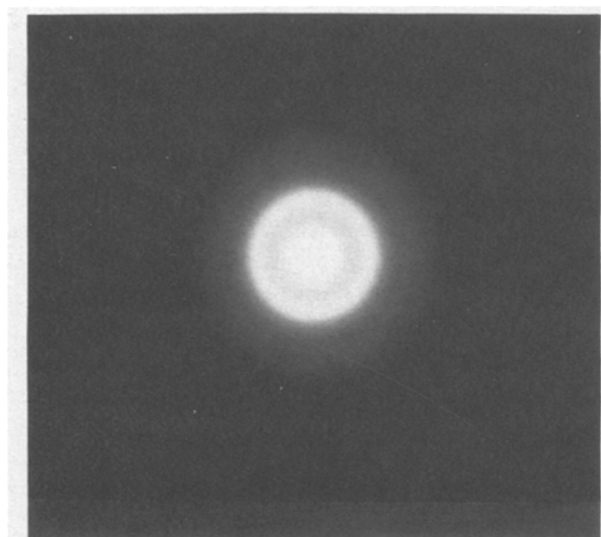
increasing N_2 flow comes as no surprise, whereas the increase in hydrogen content with higher nitrogen flow cannot be explained at this point.

MERIE etching of blanket, patterned oxide and nitride masked BN films show anisotropic etch profiles, selectivity of 13:1 for blanket (Fig. 9 and 10) and up to 25:1 (BN:nitride/oxide) for patterned films in CF_4/O_2 (90% oxygen). The etching conditions are listed in Table III, and the etch rates and selectivities are summarized in Table IV. The etch rate of BN increases with higher CF_4 flows (Fig. 9), whereas the selectivity levels out at CF_4/O_2 ratios greater than 30 (Fig. 10).

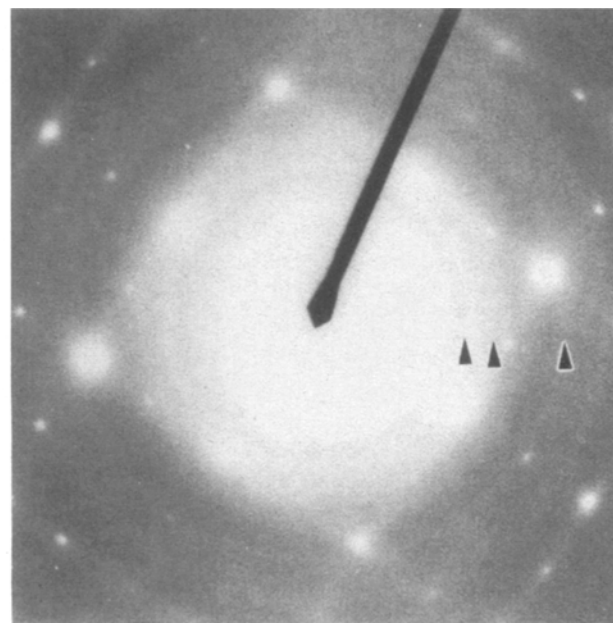
SEM analysis shows that the conformity of borazine-BN films is about 70 to 80%, whereas those of diborane-BN are about 45 to 55% over 0.7 to 1.0 μm structures with 1 to 1.2 aspect ratio (Fig. 11). For diborane-BN films, higher NH_3 flow rates enhance the conformity of the films to 55 to 70% over the same structure. A possible explanation for the better step coverage of films deposited by borazine decomposition is a more uniform sticking coefficient, and a higher surface mobility of the precursor being already in a more "complete" form. Using hydride chemistry, borazine is prepared *in situ* during the reaction sketched in Fig. 12.

FTIR analysis shows the presence of B-N bonds at various modes (B-N transverse optical mode at 700 cm^{-1} , hexagonal B-N-B vibration at 780 cm^{-1} , B-N at 910 cm^{-1} , hexagonal B-N at 1380 and 1580 cm^{-1}) together with B-H (2520 cm^{-1}) and N-H (3340 cm^{-1}) bonds,¹⁸ as shown in Fig. 13, 14. The cubic B-N bonding (TO-mode at 1050 to 1100 cm^{-1}) is only observed when borazine is used as precursor (Fig. 13).

TEM, XRD, and FTIR show differences in boron nitride bonding phases, depending on the precursor chemistries. For BN films from borazine, the average bonding lengths are B-N = 1.61 \AA (*vs.* 1.42 \AA for hexagonal, and 1.56 \AA for cubic BN), and N-N = 2.53 \AA between ring planes (*vs.* 3.33 \AA for pure hexagonal structure). This suggests a defect structure (Fig. 14) in which the ring planes (sp^2 hybrids) are linked statistically either by B-N or N-N bondings (sp^3 hy-

Hydride Chemistry BN
($\text{B}_2\text{H}_6, \text{NH}_3, \text{N}_2$)

Diborane/ Ammonia BN =
Mostly Amorphous & Hexagonal

Borazine Chemistry BN
($\text{B}_3\text{N}_3\text{H}_6, \text{N}_2$)

Borazine BN - Mixture of Hexagonal,
Wurtzite & Cubic

Fig. 16. Selected area diffraction patterns (SAED) in TEM of boron nitride layers.

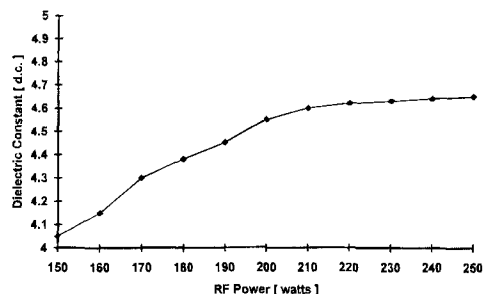


Fig. 17. Dielectric constant of BN vs. RF power (borazine chemistry).

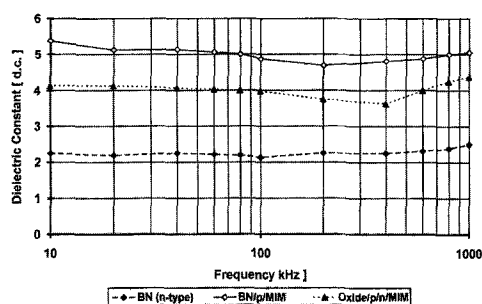


Fig. 18. Dielectric constant values of BN vs. frequency and test structure.

brids). For diborane as precursor, the films are strictly amorphous with hexagonal bonding structure. With borazine as precursor, the layers have mixed bonding conditions (amorphous, hexagonal, wurtzite, and cubic; see Fig. 13, 15). In both cases the hexagonal structure is dominant (Fig. 16). The phases confirmed are also consistent with the lower density of boron nitride films, as mentioned above.

Careful MIM and MIS capacitance measurements of layers 100 to 500 nm thick show that the d.c. values of the stable plasma CVD boron nitride films range from about 4 to 5, depending on deposition conditions (Fig. 17, 18). Boron nitride films, doped (*i.e.*, oxidized, contaminated) with oxygen have lower d.c. values but are too unstable as dielectrics due to the formation of hygroscopic B_2O_3 phases. In general, the dielectric constants of boron nitride films are strongly correlated to the composition, bonding structures, degree of crystallinity, and deposition conditions. For boron-rich boron nitride, the d.c. values are approximately 3.7 or smaller, because the boron-rich layers react in air to form both BN/ B_2O_3 phases, as in the case of oxygen-doped BN or oxygen-doped silicon boron nitride (SiBN).²⁰

It should be noted that the MIS measurement *vs.* capacitance can be misleading if n-type Si substrates are used. This is because the initial diffusion/implantation of excess boron during plasma nitride deposition, that consequently forms a p-n junction at interfaces (Fig. 18, 19). This p-n

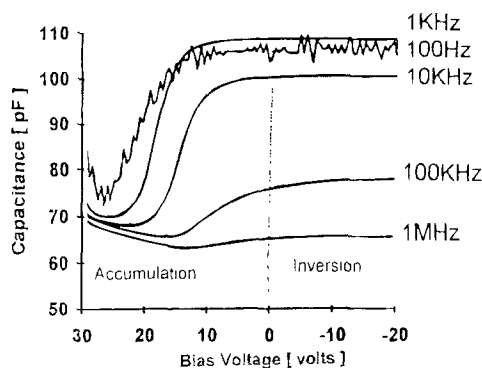


Fig. 19. p-n Junction formation effect on capacitance measurements.

junction causes inaccurate capacitance measurements and hence false d.c. calculated values.^{1,7,18} In this case, d.c. values below 3 or less may result. However, these wrong results are generally irreproducible.

Summary

Boron nitride films were deposited in a single-wafer plasma-enhanced chemical vapor deposition (PECVD) system using two different reactant chemistries. Films deposited with a 2:1 nitrogen/borazine ratio or high NH_3/B_2H_6 ratios (>5) are highly stable, nearly stoichiometric, and have low hydrogen contents in the 7 to 8 a/o range. The deposited films are amorphous with hexagonal bonding phases for diborane-BN, or of mixed hexagonal, wurtzite, and cubic nanocrystallinity for borazine-BN. Magnetically enhanced RIE with CF_4/O_2 (90% O_2) of BN films show anisotropic etch profiles, and selectivity up to 25:1 over oxide or nitride patterned films. The dielectric constant values of stable plasma boron nitride films are between 4 and 5, depending on deposition conditions.

Overall, plasma boron nitride films deposited with both chemistries under suitable conditions are stable insulators, do not react with water vapor and show promising characteristics for high density ULSI fabrication.

Acknowledgments

We acknowledge the assistances of D. Dobuzinsky, R. Gleason, M. Gibson, D. Cote, W. Hathaway, C. Basa, W. Mlynko, and D. Di Cicco of IBM, Professor W. Lanford of State University of New York at Albany, B. Neureither, R. Braun, A. Mitwalsky, G. Zorn at Siemens, P. Hefferle of PicoLab, Germany, and W. Kern, W. Kern Associates, New Jersey.

Manuscript submitted Sept. 27, 1993; revised manuscript received Jan. 20, 1994.

IBM Microelectronics assisted in meeting the publication costs of this article.

REFERENCES

1. M. Maeda and T. Makino, *Jpn. J. Appl. Phys.*, **26**, 660 (1987).
2. S. B. Hyder and T. Yep, *This Journal*, **123**, 1721 (1976).
3. W. Schmolla and H. L. Hartnagel, *ibid.*, **129**, 2636 (1982); *Solid State Electron.*, **26**, 931 (1983).
4. H. Miyamoto, M. Hirose, and Y. Osaka, *Jpn. J. Appl. Phys.*, **22**, L216 (1983).
5. K. Montasser, S. Hatori, and S. Morita, *Plasma Chem., Plasma Process*, **4**, 251 (1984); *J. Appl. Phys.*, **58**, 3185 (1985).
6. I. Yuzuriha, D. Hess, and W. Mlynko, *J. Vac. Sci. Technol.*, **A3**, 2125 (1985); *Thin Solid Films*, **140**, 199 (1986).
7. M. Maeda, T. Makino, E. Yamamoto, and S. Konaka, *IEEE Trans. Electron Devices*, **ED-36**, 1610 (1989).
8. J. Kouvetakis, V. V. Patel, C. W. Miller, and D. B. Beach, *J. Vac. Sci. Technol.*, **A36**, 3929 (1990).
9. O. Gafri, A. Grill, D. Itzhak, A. Inspektor, and R. Avni, *Thin Solid Films*, **72**, 523 (1980).
10. S. P. S. Ayra and A. D'Amico, *ibid.*, **157**, 267 (1988).
11. O. S. Poon, A. Gelatos, A. H. Perera, and M. Hoffman, Abstract 8, p. 115, 1993 *VLSI Technology Symposium*, **B-5** (1993).
12. S. V. Nguyen, D. Dobuzinsky, D. Harmon, S. Fridmann, and R. Gleason, *This Journal*, **137**, 2209 (1990).
13. Scofield Table, *J. Electron. Spectrosc.*, **8**, 129 (1976).
14. W. A. Lanford and M. J. Rand, *J. Appl. Phys.*, **49**, 2473 (1978).
15. S. V. Nguyen, D. Dobuzinsky, and D. Harmon, *Solid State Technol.*, **10**, 73 (1990).
16. P. H. Pan, J. Abernathy, and C. Schaefer, *J. Electron Mater.*, **14**, 617 (1985).
17. *CRC Handbook of Chemistry and Physics*, R. C. Weast, Editor, CRC Press, Boca Raton, FL (1976-1977).
18. M. Maeda, *Mater. Res. Soc. Symp. Proc.*, **284**, 457 (1992).
19. A. Weber, U. Bringmann, R. Nikulski, and C. P. Klages, in *Proceedings of Diamond Conference, Germany*, Session 7.3 (1993).
20. M. Maeda, *Jpn. J. Appl. Phys.*, **29**, 1789 (1990).